Improved Detection of Distorted IR-UWB Pulses Using Amplitude Spectrum in Indoor Environments

Thorsten Wehs, Gerd von Cölln, Carsten Koch, Tilman Leune
Hochschule Emden/Leer, University of Applied Sciences, Germany
Department of Informatics and Electronics
Email: {thorsten.wehs | gerd.von.coelln | carsten.koch| tilman.leune}@hs-emden-leer.de

***Abstract*—In dense environments, such as residential, office or industrial sites, the predominant type of link encountered by a radio based real-time localization system (RTLS) is non-line-of-sight (NLOS). Often, the mobile nodes are separated from their related anchor nodes by the building's walls. In Impulse Radio Ultra Wideband (IR-UWB) based localization systems, the penetration of walls can cause significant distortions of the pulses. The grade of distortion depends on the walls' thickness, materials used and the pulses' angle of incidence.**

Pulse distortion has a negative impact on the performance of correlation in matched filter (MF) based algorithms in the time domain. This paper presents a detailed evaluation of an approach using the amplitude spectrum of the received signal for correlation. To evaluate this approach, simulations were performed for typical materials of walls, with varying wall thicknesses and angles of incidence and, in addition, different pulse types according to the regulations. For the parameter space using an UWB pulse with bandwidth compliant to FCC, improvements up to 15 % were reached.

I. Introduction

Localization systems providing a high resolution and good accuracy over a wide area are a key requirement for Smart Factories, Cyber-Physical Systems and Industry 4.0 in general.

Highly precise satellite based locating solutions (GNSS, global navigation satellite system) are available for a broad array of outdoor applications. Custom of-the-shelf (COTS) realtime localization systems (RTLS) for indoor use employing several different technologies are also available. The approach of employing Ultra Wideband (UWB) radio to track mobile nodes attached to entities has been shown to perform with high accuracy [1, 2]. Since UWB does transmit very short pulses instead of modulating a carrier wave, the achievable ranging accuracy surpasses that of other radio technologies. A drawback of currently available UWB ranging solutions is the need for line-of-sight (LOS) or weak non-line-of-sight (NLOS) links since obstacles between transmitter and receiver negatively impact the maximum reachable accuracy. To circumvent this limit, the canonical solution would be to place more anchor nodes, which is not feasible for all applications and environments.

Typical residential, industrial or office environments tend to be very dense, so the majority of radio links in such an environment will be NLOS [3]. The UWB pulses are able to penetrate many of the construction materials which are typically present in obstacles such as walls or doors, but this introduces a bias in the resulting range estimation [4, 5]. Additionally, the received pulses' shape will be distorted and the received signal strength does suffer from significant attenuation.

The distortion is a peculiarity of pulse based radio technologies. Due to the wide bandwidth, there is a wide range of frequencies affected by the penetration of walls, for example. One cause for the distortion is that each frequency component has an individual relative phase shift depending on the material, angle of incidence and thickness of the wall.

In case of radio receivers based on matched filter (MF) algorithms, the performance is degraded in accordance to the grade of pulse distortion.

A. Motivation

The aim of the paper is to present a detailed evaluation of a new approach for the detection of distorted UWB pulses in radio receivers, which is already published by the authors in [6]. In addition the mentioned paper encloses an improved receiver algorithm based on this new approach.

The motivation is to improve the performance of pulse detection in NLOS-afflicted indoor localization. Basis for the new approach is the detection of pulses in frequency domain, more precisely using the amplitude spectrum of the signals. In this regard, a main aspect is to show the impact of penetration effects on the propagation of UWB pulses through walls.

A common scenario for indoor localization is a set of anchor nodes distributed in a building. Fig. 1 depicts a typical geometry of such a localization scenario. The anchor nodes are distributed in the rooms and hallways. Typically within a localization process of a mobile node there is a mix of LOS and NLOS links (see Fig. 1). The type and grade of pulse distortion depends on the angle of incidence of the pulse at the wall in combination with the material and thickness thereof. Regarding the mentioned typical scenarios, this paper will provide a quantification of the improvement and therefore the potentialities and the limitations of the proposed approach.

B. Related work

There are several approaches for the detection of the first incoming pulse or the leading edge in time-of-flight (ToF) measurements, which differ in terms of complexity and reliability. For example threshold-based leading-edge detection (Th-LED) on the received signal (waveform) [7] or a further enhancement by applying two centralized average filters to

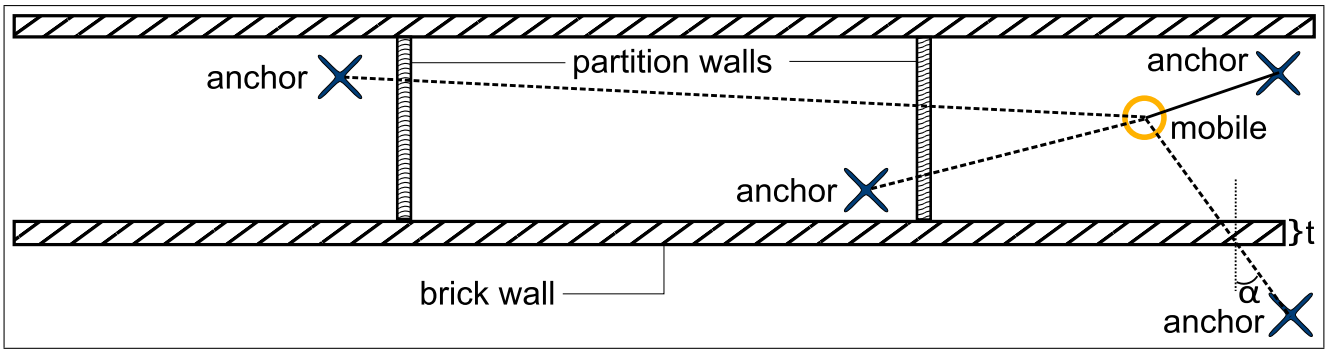

Fig. 1: Exemplary and schematic view on an indoor localization scenario e. g. in an office environment. The range measurements undergo penetration effects due to the walls within the buildung.

the signal (adaptive LED) [8]. Many of them are based on the matched filter (MF) signal which is typically a correlation with the transmitted pulse template in time domain. Those algorithms could be improved by applying the proposed approach.

A lot of research has been done on the quantification of the bias error due to penetration effects [9, 10, 11] and further on the effect onto localization reliability and accuracy [12]. On the way to this, the frequency dependent parameters were investigated for typical building materials which can be found in [13] or [14]. But extensive studies on the mitigation of pulse distortion effects are still missing.

The following sections of this paper are structured as follows: In Sec. II the new approach for detection of distorted pulses based on amplitude spectrum analysis, is presented. The simulational results and the performance of the proposed approach are shown in Sec. III. Sec. IV concludes the paper with an additional outlook.

II. Correlation in Frequency Domain

The proposed approach is based on the observation that in many cases the amplitude spectrum of an UWB pulse is weaker affected due distortion than the phase spectrum. Therefore, the idea is to take solely the amplitude spectrum of the received signal for the pattern matching by correlation. This method is called |F|-correlation in following.

The mathematical model for a discrete UWB pulse is:

$$s[t] = A \cdot \left(1 - \frac{4\pi(t-T_c)^2}{\tau^2}\right) \cdot \exp^{-\frac{2\pi(t-T_c)^2}{\tau^2}} \tag{1}$$

where A is the amplitude of the pulse, T_c the offset on time axis and τ the characteristic time constant of the UWB pulse [14].

In many localization scenarios, the ideal transmitted pulse $s[t]$ (or $\boldsymbol{s}$) is distorted in its shape and attenuated in its amplitude by a NLOS link. Hence, the distorted first pulse $s_{d1}[t]$ (or $\boldsymbol{s_{d1}}$) is, among others, e. g. multi path components and noise, element of the received waveform $r[t]$.

In [14] the impact of the NLOS case *penetration of a dielectric slab* is described. This NLOS case will be the overall focus of the following considerations. Decisive part of the pulse distortion is the relative shift of the containing frequency components. In this cases the pulses phase spectrum is more affected than the pulses amplitude spectrum. In conjunction to that, the coefficients from |F|-correlation will be higher than those from correlation in the time domain where amplitude and phase are combined (further called t-correlation). The correlation coefficient in time domain ρ_t can be described as the Pearson Correlation Coefficient (PCC):

$$\rho_t = \left| \frac{n_t(\boldsymbol{s} \cdot \boldsymbol{s_{d1}}) - (\sum \boldsymbol{s})(\sum \boldsymbol{s_{d1}})}{\sqrt{[n_t(\boldsymbol{s} \cdot \boldsymbol{s}) - (\sum \boldsymbol{s})^2][n_t(\boldsymbol{s_{d1}} \cdot \boldsymbol{s_{d1}}) - (\sum \boldsymbol{s_{d1}})^2]}} \right| \tag{2}$$

where n_t is the length of the pulses, $\boldsymbol{s}$ the transmitted pulse and $\boldsymbol{s_{d1}}$ the received distorted pulse in time domain. To compare the correlation coefficients, the absolute value of the PCC is used.

The equivalent PCC correlation in frequency domain ρ_f can be determined as:

$$\boldsymbol{a_s} = a_s[\omega] = |\text{dft}(\boldsymbol{s})| \tag{3}$$

$$\boldsymbol{a_{s_{d1}}} = a_{s_{d1}}[\omega] = |\text{dft}(\boldsymbol{s_{d1}})| \tag{4}$$

$$\rho_f = \left| \frac{n_f(\boldsymbol{a_s} \cdot \boldsymbol{a_{s_{d1}}}) - (\sum \boldsymbol{a_s})(\sum \boldsymbol{a_{s_{d1}}})}{\sqrt{[n_f(\boldsymbol{a_s} \cdot \boldsymbol{a_s}) - (\sum \boldsymbol{a_s})^2][n_f(\boldsymbol{a_{s_{d1}}} \cdot \boldsymbol{a_{s_{d1}}}) - (\sum \boldsymbol{a_{s_{d1}}})^2]}} \right| \tag{5}$$

where n_f is the width of the spectrums $\boldsymbol{a_s}$ and $\boldsymbol{a_{s_{d1}}}$ (typically $n_f = 2^p \geq n_t, p \in \mathbb{N}$), $\boldsymbol{a_s}$ the amplitude spectrum of the transmitted and $\boldsymbol{a_{s_{d1}}}$ the amplitude spectrum of the received pulse. To compare the correlation coefficients, the absolute value of the PCC is used. For better readability, Eqn. 5 is equivalent to:

$$\rho_f = |\text{pcc}(\boldsymbol{a_s}, \boldsymbol{a_{s_{d1}}})| \tag{6}$$

According to the circumstance that correlating amplitude spectrums outperforms correlation in time domain, the condition for an improved detection result is:

$$\rho_f > \rho_t \tag{7}$$

In the next section the theoretical improvement of the pulse correlation in frequency domain will be quantified with some typical examples in several experimental setups.

III. Simulations and Performance

Aim of the simulations is to quantify the absolute improvement of |F|-correlation against t-correlation. This will be done by simulating the distortion for different materials used for walls. The angle of incidence on the surface of the wall is varied in a range of $0\,^\circ$ to $75\,^\circ$ and the thickness is varied from $0\,\text{cm}$ to $25\,\text{cm}$. The actual distortion is calculated as described by Jing et al. in [10]. Values for the frequency dependent material parameters dielectric constant ϵ_r and loss tangent $\tan\delta$ from $2\,\text{GHz}$ to $11\,\text{GHz}$ are taken from that publication, too (see Fig. 3).

In the following subsections two representative pulse templates are analysed: one with a large bandwidth and another with a smaller bandwidth. The pulse with the large bandwidth is exemplifying for the compliance to the regulations of Federal Communications Commission (FCC) (cf. Fig. 2). Regulations from European Electronic Communications Committee (ECC) are more restrictive and allow only about $2\,\text{GHz}$ in two different frequency ranges (cf. Fig. 2).

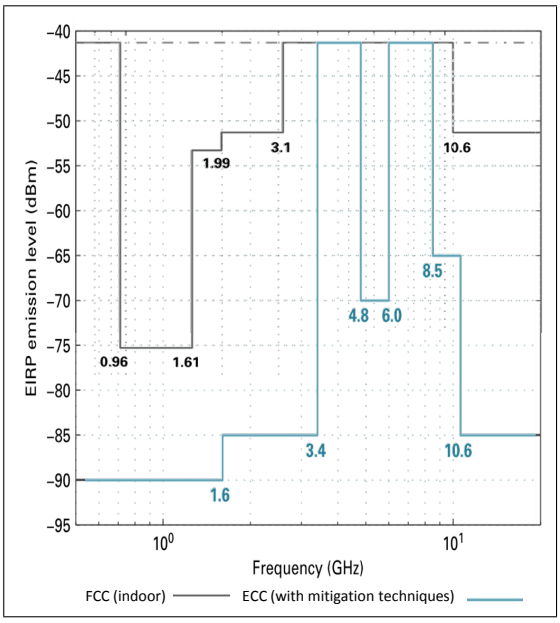

Fig. 2: UWB regulations FCC and ECC (cf. [15]).

A. Pulse template with 9 GHz bandwidth

For the first considered pulse template, which uses most of the bandwidth from $2\,\text{GHz}$ to $11\,\text{GHz}$ for which material parameters are available, we are using the parameters: $T_c = 0\,\text{ns}$ and $\tau = 0.134\,\text{ns}$ for pulse generation (cp. Eqn. 1). In our consideration the absolute amplitude A of the pulse is irrelevant. The resulting pulse template is shown for example in the upper subplots in Fig. 5 (blue line/marker). The pulses are represented by 61 samples with a sample interval of $15.625\,\text{ps}$ ($f_s = 64\,\text{GHz}$).

Fig. 4 shows the performance of the |F|-correlation against t-correlation for material type *brick*. The x-axis of the surface plot shows the thickness of the wall (stepsize $1\,\text{cm}$) and the y-axis shows the angle of incidence of the pulse (stepsize $3\,^\circ$). The colour of the elements represent the ratio of the correlation coefficients $\eta_{m,t,\alpha}$ (cf. Eqn. 2 and 5) calculated as follows:

$$\eta_{m,t,\alpha} = 1 - \frac{\rho_{t_{m,t,\alpha}}}{\rho_{f_{m,t,\alpha}}} \tag{8}$$

where m is the type of material, t the thickness of the wall and α the angle of incidence. The coefficient $\rho_{t_{m,t,\alpha}}$ is the maximum value of a cross-correlation of the pulse template and the distorted pulse (e. g. blue and red line in the upper subplot in Fig. 5a). In addition the two signal segments are synchronized at this maximum correlation coefficient in the comparison plots. The $\rho_{f_{m,t,\alpha}}$ are calculated with the corresponding amplitude spectrums which are shown in the lower subplots in Fig. 5.

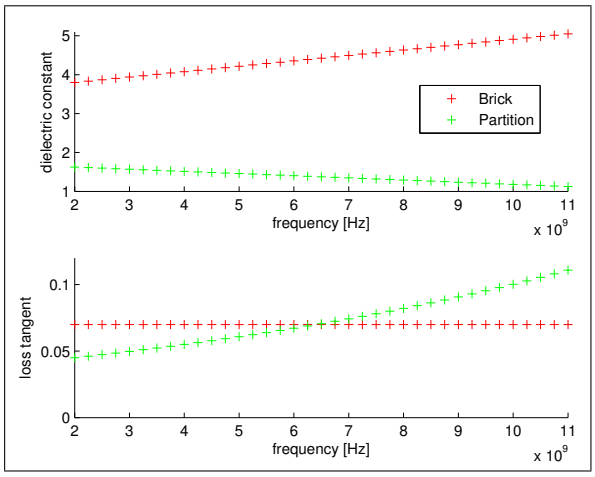

Fig. 3: Frequency dependent material constants dielectric constant ϵ_r and loss tangent $\tan\delta$ for materials brick and partition (cf. [10]).

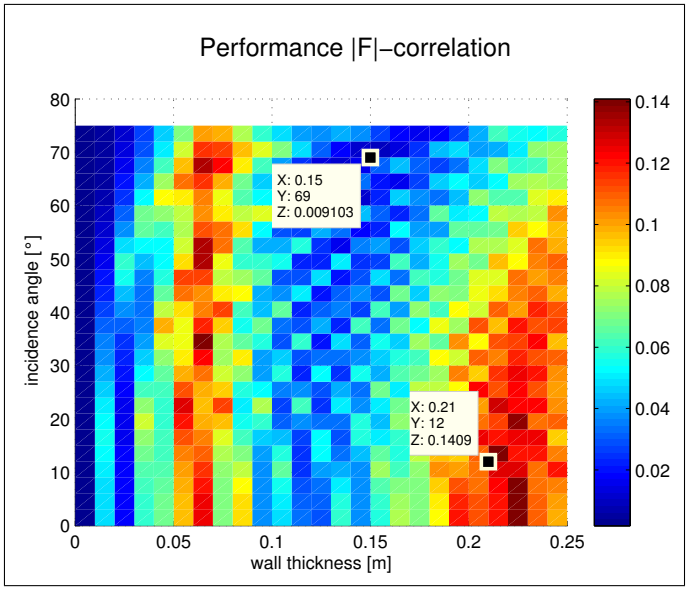

Fig. 4: Surface plot of the correlation ratio between |F|- and t-correlation over the wall thickness and the angle of incidence for material type *brick* and $9\,\text{GHz}$ bandwidth.

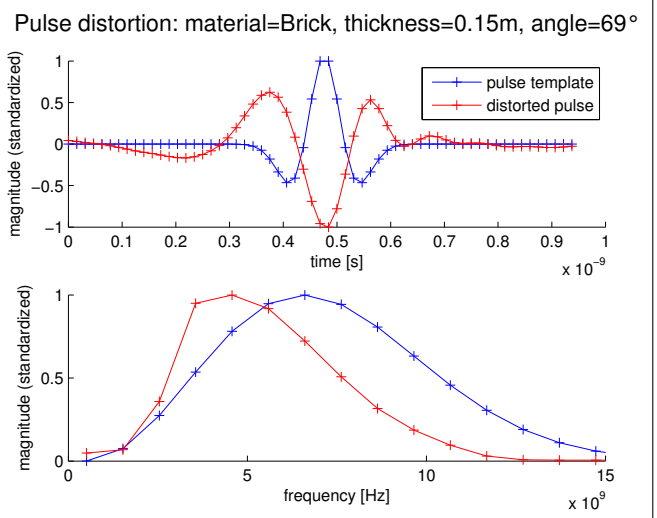

(a) wall thickness of 15 cm and angle of incidence of 69 ° resulting in performance ratio $\eta_{\text{brick},15\,\text{cm},69\,\circ}$ of 0.009

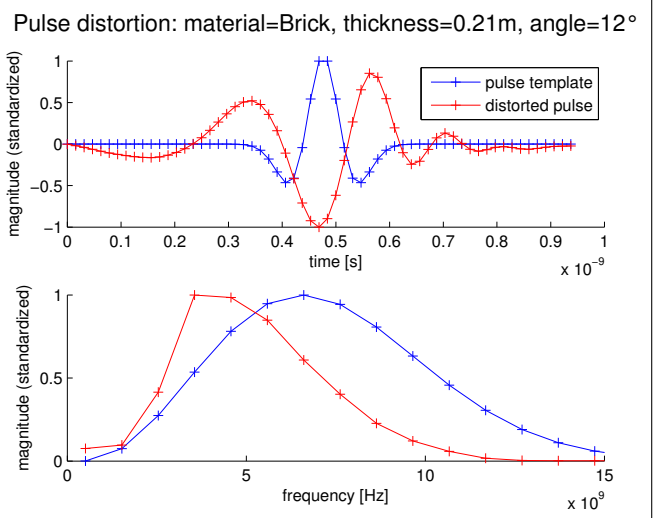

(b) wall thickness of 21 cm and angle of incidence of 12 ° resulting in performance ratio $\eta_{\text{brick},21\,\text{cm},12\,\circ}$ of 0.141

Fig. 5: Comparison of the pulse template (blue) and the pulse distorted by a wall of brick (9 GHz bandwidth).

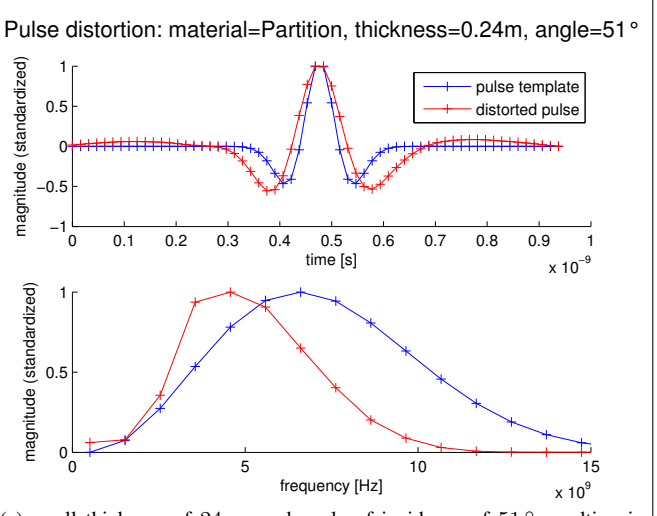

(a) wall thickness of 24 cm and angle of incidence of 51 ° resulting in performance ratio $\eta_{\text{partition},24\,\text{cm},51\,\circ}$ of -0.056

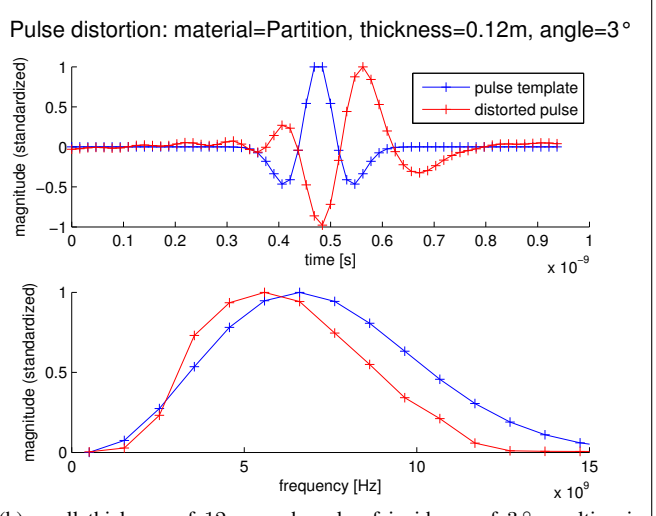

(b) wall thickness of 12 cm and angle of incidence of 3 ° resulting in performance ratio $\eta_{\text{partition},12\,\text{cm},3\,\circ}$ of 0.136

Fig. 6: Comparison of the pulse template (blue) and the pulse distorted by a wall of partition (9 GHz bandwidth).

It can be seen in Fig. 4 that the improvement of applying |F|-correlation varies from 0 % to about 14 % in this test range, with this pulse type and brick as material. In addition there is a very irregular distribution of higher and lower correlation ratio values $\eta_{m,t,\alpha}$ visible. The pattern and the absolute values for $\eta_{m,t,\alpha}$ are dependent of the material parameters and the type of pulse template. It is noticeable that the impact of the angle on the distortion is not very strong in this test case. There is only slight alteration from 20 cm wall thickness visible.

Fig. 5a shows an exemplary comparison of a distorted pulse with a very small $\eta_{m,t,\alpha}$. In this case the reason is a similar grade of distortion in time domain ($\rho_{t_{m,t,\alpha}}$) and of the amplitude spectrum ($\rho_{f_{m,t,\alpha}}$). On the other hand in Fig. 5b is shown an example where correlation in frequency domain clearly outperforms the traditional correlation in time domain.

For material *partition*, there is a totally different pattern of performance (see Fig. 7). In comparison to the pattern of material brick (Fig. 4) there is a stronger dependency of the angle of incidence. Furthermore there is an area from 20 cm to 25 cm and 40 ° to 60 ° where the performance $\eta_{m,t,\alpha}$ is degraded to zero respectively turns to negative. An example for this negative ratio is depicted in Fig. 6a. Despite the high values for thickness and angle of incidence, the pulse is not deformed as much as expected. The pulse in time domain is

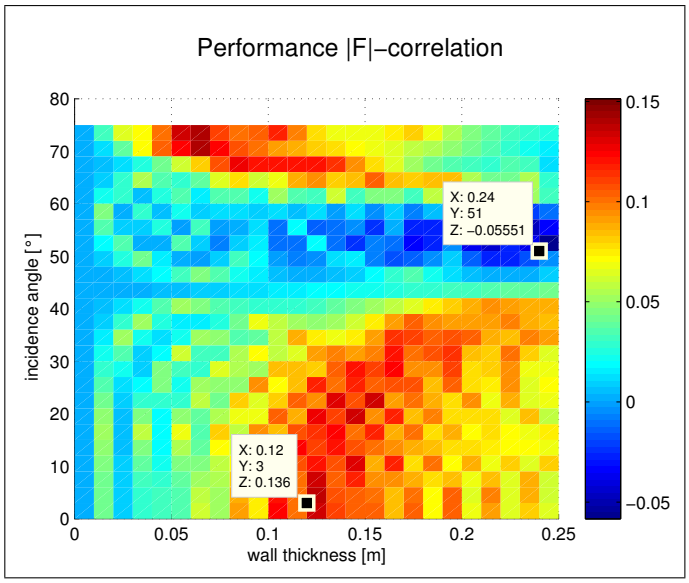

Fig. 7: Surface plot of the correlation ratio between |F|- and t-correlation over the wall thickness and the angle of incidence for material type *partition* and 9 GHz bandwidth.

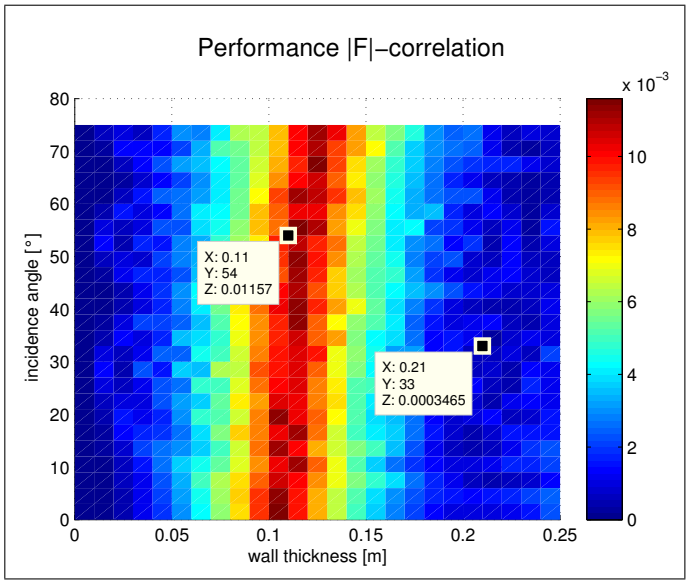

Fig. 8: Surface plot of the correlation ratio between |F|- and t-correlation over the wall thickness and the angle of incidence for material type *brick* and 2.2 GHz bandwidth.

distorted in a manner that the left and right tail have a proper proportion and there is only a slight overall stretch in the time-axis. In the amplitude spectrum the higher frequencies are stronger attenuated so there is a visual shift of the magnitude maximum to the lower frequencies.

To sum up, the maximum value of the whole matrix is in the same order as with material brick. An exemplifying distortion with a higher performance of about 13.6 % is shown in Fig. 6b. There the tails of the pulse in time domain are partially shrunk and stretched. So the pulse is strongly distorted and the $\eta_{m,t,\alpha}$ rises.

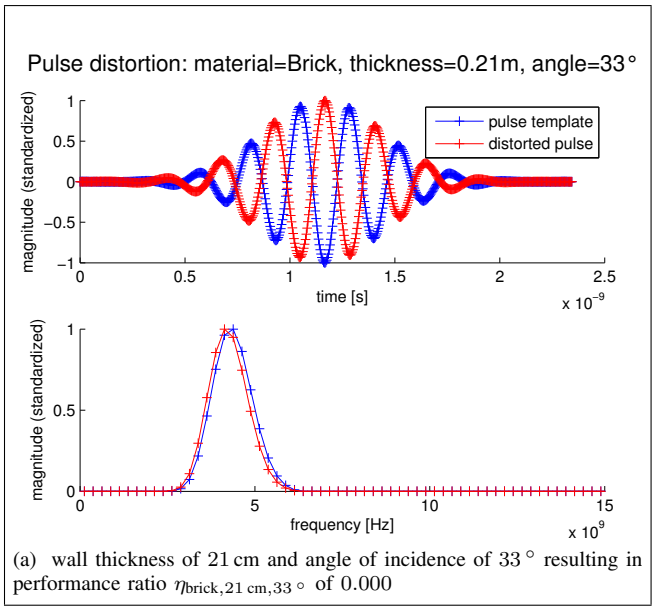

(a) wall thickness of 21 cm and angle of incidence of 33 ° resulting in performance ratio $\eta_{\text{brick},21\,\text{cm},33\,\circ}$ of 0.000

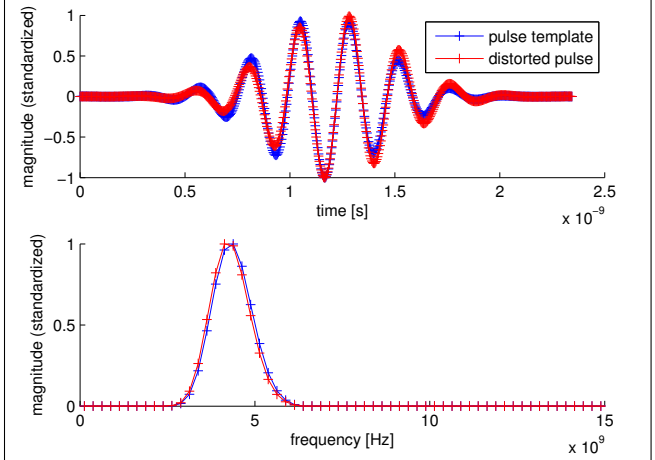

(b) wall thickness of 11 cm and angle of incidence of 49 ° resulting in performance ratio $\eta_{\text{brick},11\,\text{cm},45\,\circ}$ of 0.012

Fig. 9: Comparison of the pulse template (blue) and the pulse distorted by a wall of brick (2.2 GHz bandwidth).

B. *Pulse template with 2.2 GHz bandwidth*

A further important question is the impact of the bandwidth on the distortion. In the previous subsection, a pulse with a high bandwidth was considered. Now, a much smaller bandwidth is analysed. We took a pulse template, which uses only a bandwidth of 2.2 GHz. It is generated with the parameters: $T_c = 0$ ns and $\tau = 0.7$ ns. The pulse was shifted in frequency domain up to a range from 3.1 GHz to 5.3 GHz. This type of pulse is used for example in UWB transceivers manufactured by the company Time Domain (cf. [16]). The pulse is sampled with a shorter interval of about 3.906 ps ($f_s = 256$ GHz), because of the more detailed pulse shape. Due to the smaller bandwidth the pulse is wider than the previous template in time domain. The pulses are cut out and represented due 601

sample values (cf. Fig. 9a and 9b).

In Fig. 8 the performance of the |F|-correlation $\eta_{m,t,\alpha}$ with the small bandwidth pulse is depicted. There is an influence of the thickness observable, whereas the angle of incidence has no significant impact on the performance in this test case. But in fact the overall performance is very weak. Even the high values around a wall thickness of 10 cm are only about $1\,\%$ improvement due |F|-correlation. Fig. 9a is an example for a weak performance despite higher values for thickness and angle. The pulse is inverted in time domain, but neither the shape in time domain nor the amplitude spectrum is distorted significantly. Also in the case of a better performance (e. g. Fig. 9b) the shape and the spectrum are both only slightly distorted. This results in generally low values for the performance of lesser than $1.1\,\%$ in this test case.

This shows that the bandwidth of the UWB pulse is an important criterion for the grade of distortion and therefore for the performance of |F|-correlation.

IV. Conclusion

In indoor environments UWB pulses are often strongly distorted and attenuated by the penetration of walls or other obstacles. This paper presented the detailed evaluation of an approach for the improved detection of distorted UWB pulses for ToF measurements. The approach is to detect the distorted pulses on the basis of the amplitude spectrum instead with the established way in time domain. The idea based on the assumption that in many NLOS cases with penetration effects, the phase spectrum is more strongly affected than the amplitude spectrum. Therefore a correlation based on the amplitude spectrum outperforms a correlation in time domain.

The results in Sec. III show that this applies only in some cases and depends on the bandwidth of the pulse template and the penetrated material. The approach performs well with the use of pulse templates with a large bandwidth. With the analysed parameter space improvements up to $15\,\%$ were reached in our simulations. But in small bandwidth systems only an insignificant improvement of about $1\,\%$ was reached.

Next step is an real world evaluation of the simulated results from this and the previous paper [6]. Due to distortion of the pulse, the maximum value of t-correlation is often not longer centralized to the middle of the pulse. Therefore a further step is to examine if, there is a positive impact to a centralized detection of the distorted pulse in |F|-correlation by a sliding DFT.

Acknowledgment

The authors would like to thank the European Regional Development Fund (ERDF) and state of Lower Saxony to give us the possibility to research at such an interesting and innovative subject.

References

[1] T. Phebey, "The Ubisense Assembly Control The Ubisense Assembly Control Solution for BMW," in *RTLS in Manufacturing Workshop - RFID Journal Europe Live!*, 2010.

[2] Zebra Technologies, Ed., *Zebra Dart Ultra-Wideband Brochure*, 2010.

[3] Maranò, S., W. Gifford, H. Wymeersch, and M. Win, "NLOS identification and mitigation for localization based on UWB experimental data," *IEEE Journal on Selected Areas in Communications*, vol. 28, no. 7, 2010.

[4] D. Dardari, A. Conti, U. Ferner, A. Giorgetti, and M. Win, "Ranging With Ultrawide Bandwidth Signals in Multipath Environments," *Proceedings of the IEEE*, vol. 97, no. 2, pp. 404–426, 2009.

[5] C. Chen, D. Hong, H. Xiaotao, L. Xiangyang, and Y. Jibing, "Through-wall localization with UWB sensor network," in *Ultra-Wideband (ICUWB), 2012 IEEE International Conference on*, 2012, pp. 284–287.

[6] T. Wehs, T. Leune, G. v. Cölln, and C. Koch, "Detection of Distorted IR-UWB Pulses in Low SNR NLOS Scenarios," *IEEE International Conference on Ultra-WideBand (ICUWB), Paris*, 2014.

[7] K. Haneda, K. i. Takizawa, J. i. Takada, M. Dashti, and P. Vainikainen, "Performance evaluation of threshold-based UWB ranging methods - Leading edge vs. search back -," in *Antennas and Propagation, 2009. EuCAP 2009. 3rd European Conference on*, 2009, pp. 3673–3677.

[8] M. Kuhn, J. Turnmire, M. Mahfouz, and A. Fathy, "Adaptive leading-edge detection in UWB indoor localization," in *Radio and Wireless Symposium (RWS), 2010 IEEE*, 2010, pp. 268–271.

[9] Khajitpan Makaratat, Tim Brown, Stavros Stavrou, and Barry Evans, "Classification of UWB Multipath Clusters and Its Distortion Effects on Positioning Error."

[10] M. Jing, Y. Z. Qin, and T. Z. Nai, "Impact of IR-UWB waveform distortion on NLOS localization system," in *Ultra-Wideband, 2009. ICUWB 2009. IEEE International Conference on*, 2009, pp. 123–128.

[11] P. Protiva, J. Mrkvica, and J. Macháč, "Time delay estimation of UWB radar signals backscattered from a wall," *Microwave and Optical Technology Letters*, vol. 53, no. 6, pp. 1444–1450, 2011.

[12] D. Dardari, A. Conti, J. Lien, and M. Z. Win, "The Effect of Cooperation on UWB-Based Positioning Systems Using Experimental Data," *EURASIP Journal on Advances in Signal Processing*, vol. 2008, no. 1, p. 513873, 2008.

[13] A. Muqaibel, A. Safaai-Jazi, A. Bayram, A. Attiya, and S. Riad, "Ultrawideband through-the-wall propagation," *IEE Proceedings - Microwaves, Antennas and Propagation*, vol. 152, no. 6, p. 581, 2005.

[14] M. Jing, Z. Nai-tong, and Z. Qin-yu, "IR-UWB Waveform Distortion Analysis in NLOS Localization System," *Information Technology Journal*, vol. 9, no. 1, pp. 139–145, 2010.

[15] Z. Şahinoğlu, S. Gezici, and I. Güvenç, *Ultra-wideband positioning systems: Theoretical limits, ranging algorithms, and protocols*. Cambridge and UK and and New York: Cambridge University Press, 2008.

[16] Time Domain, *Data Sheet PulsON P400 RCM*, 2011.